

Supplementary Materials

Laser induced white emission generation from $\text{La}_{1-x}\text{Nd}_x\text{AlO}_3$ nanocrystals

J. M. Goncalves, M. Stefanski, R. Tomala, A. Musialek and W. Strek.

Institute of Low Temperature and Structure Research,

Polish Academy of Sciences, 50-422 Wroclaw, Poland

corresponding author: j.goncalves@intibs.pl

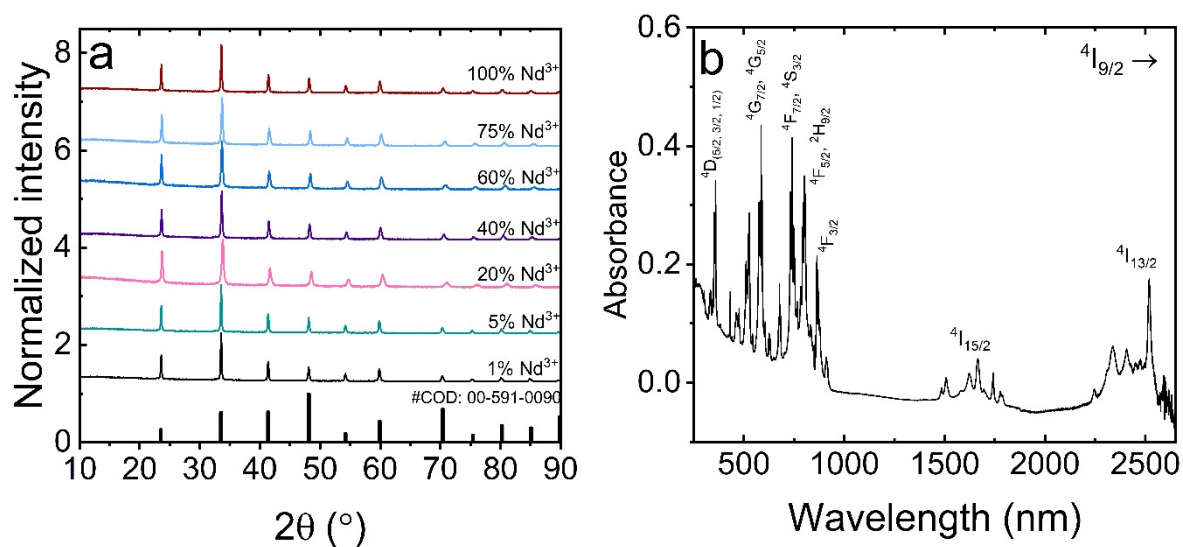


Fig. S1. Powder XRD of $\text{La}_{1-x}\text{AlO}_3:x\text{Nd}^{3+}$ perovskites (a) and diffuse reflectance spectra of NdAlO_3 (b).

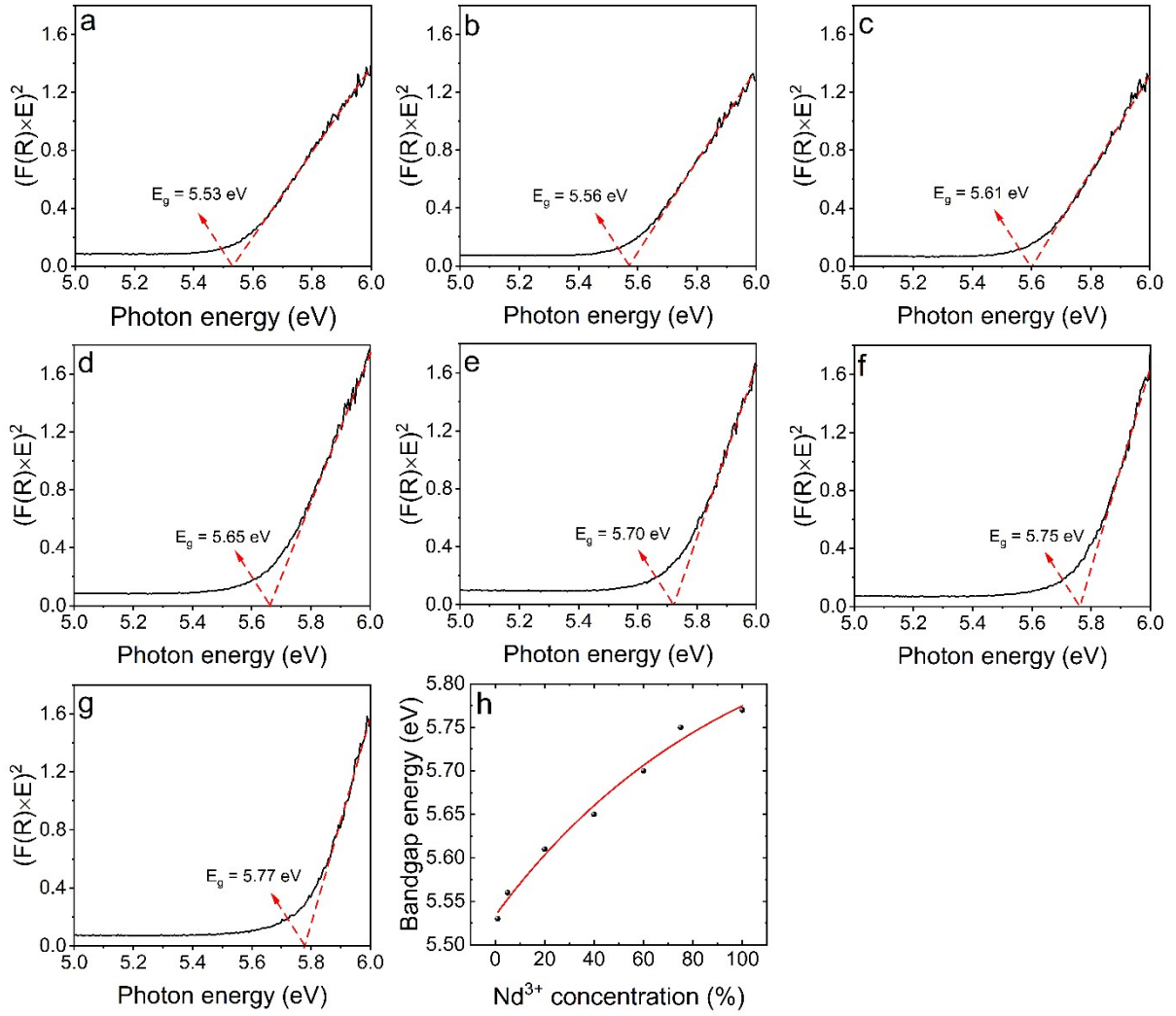


Fig. S2. Tauc plots for bandgap energy calculations of (a) $\text{LaAlO}_3:1\%\text{Nd}^{3+}$, (b) $\text{LaAlO}_3:5\%\text{Nd}^{3+}$, (c) $\text{LaAlO}_3:20\%\text{Nd}^{3+}$, (d) $\text{LaAlO}_3:40\%\text{Nd}^{3+}$, (e) $\text{LaAlO}_3:60\%\text{Nd}^{3+}$, (f) $\text{LaAlO}_3:75\%\text{Nd}^{3+}$, (g) NdAlO_3 and (h) the correlation of the bandgap energy with Nd^{3+} concentration.

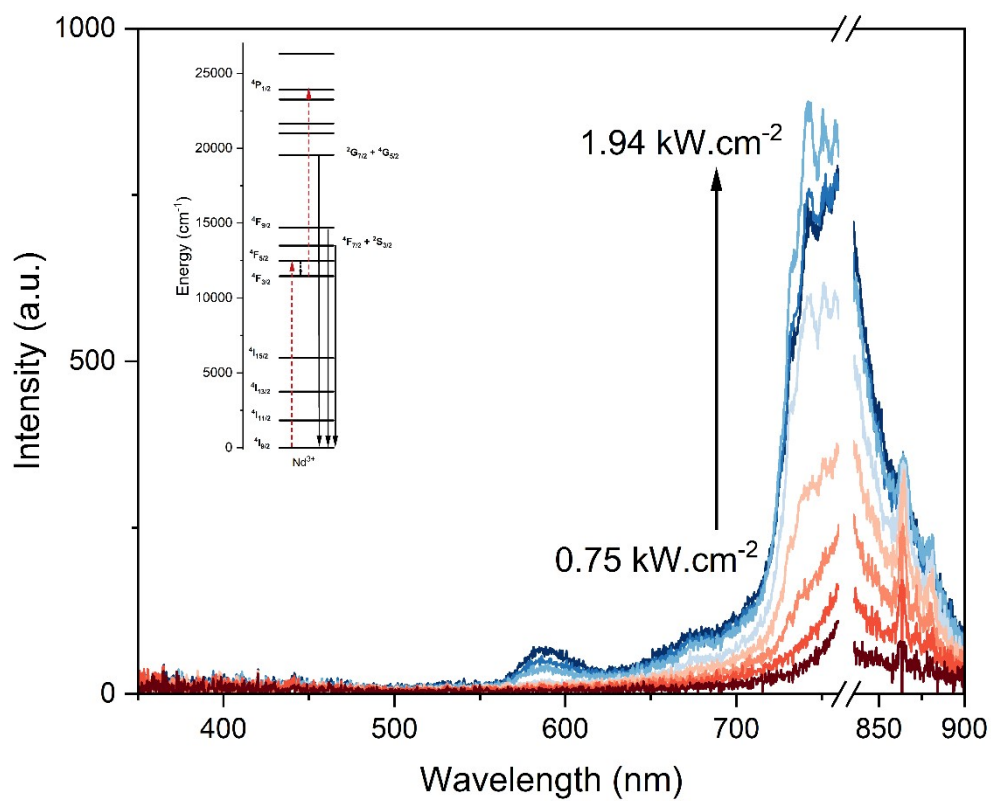


Fig. S3. Emission spectra of $\text{LaAlO}_3:1\%\text{Nd}^{3+}$ at low power excitation showing 2 photon upconversion. Inset: Simplified energy level diagram containing relevant energy levels.

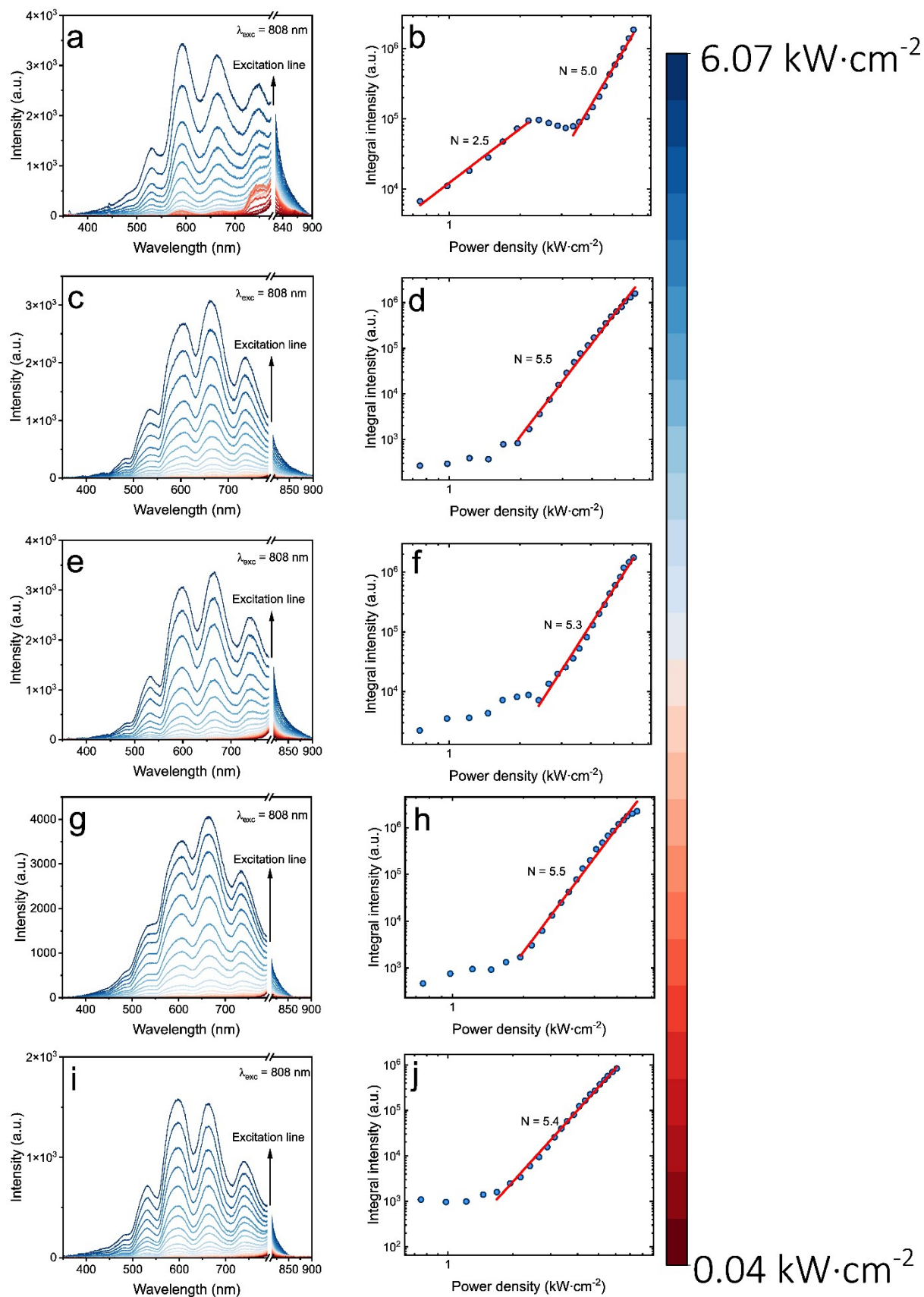


Fig. S4. Power dependence of $\text{LaAlO}_3:5\text{Nd}^{3+}$ (a-b), $\text{LaAlO}_3:20\text{Nd}^{3+}$ (c-d), $\text{LaAlO}_3:40\text{Nd}^{3+}$ (e-f), $\text{LaAlO}_3:60\text{Nd}^{3+}$ (g-h) and $\text{LaAlO}_3:75\text{Nd}^{3+}$ (i-j).

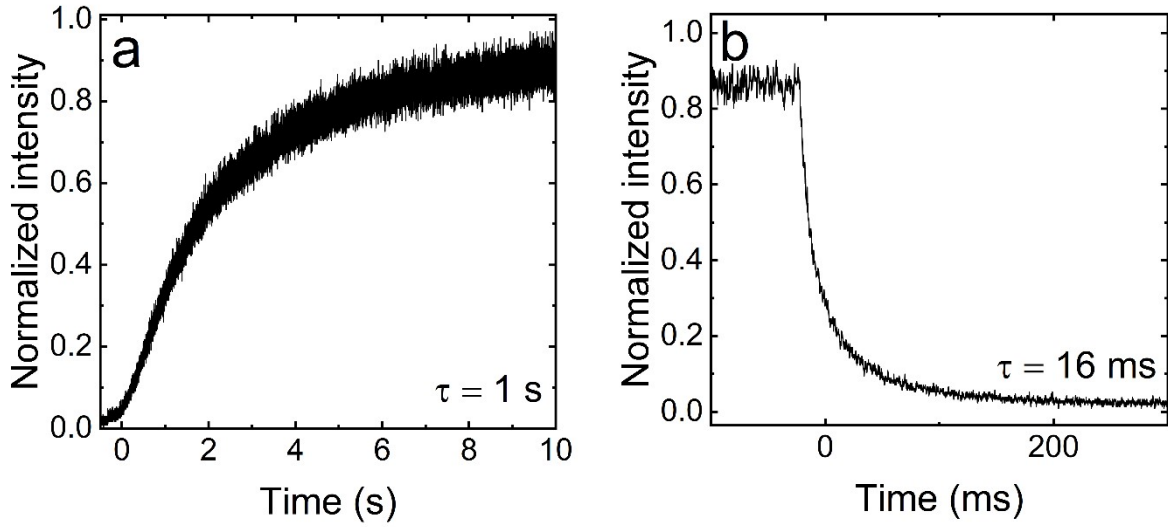


Fig. S5. Rise (a) and decay (b) times for NdAlO₃.

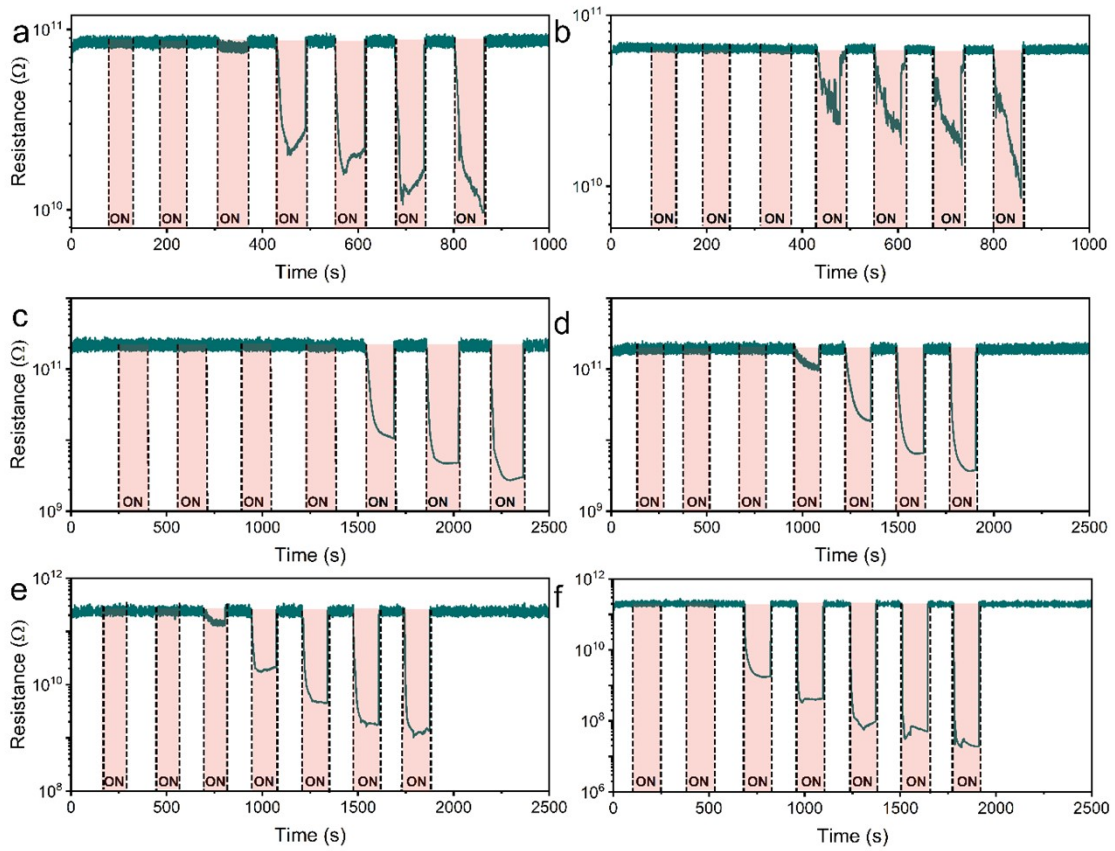


Fig. S6. Photoresistance of LaAlO₃:1%Nd³⁺ (a), LaAlO₃:5%Nd³⁺ (b), LaAlO₃:20%Nd³⁺ (c), LaAlO₃:40%Nd³⁺ (d), LaAlO₃:60%Nd³⁺ (e) and LaAlO₃:75%Nd³⁺ (f) with 1 minute on/off cycles.

Table S1. Correlated color temperature (CCT) of the emission for $\text{La}_{1-x}\text{Nd}_x\text{AlO}_3$

Nd³⁺ content	CCT (K)
0	2120
1	2111
5	2355
20	2307
40	2261
60	2366
75	2441
100	2354